C. R. Physique 13 (2012) 410–425

Contents lists available at SciVerse ScienceDirect

Comptes Rendus Physique

www.sciencedirect.com

Advances in nano-electromechanical systems

Interplay of magneto-elastic and polaronic effects in electronic transport through suspended carbon-nanotube quantum dots

Influence des effets magnéto-élastique et polaronique sur le transport électronique à travers un point quantique formé avec un nanotube de carbone suspendu

G. Rastelli [a], M. Houzet [b], L. Glazman [c], F. Pistolesi [d,e,*]

[a] *Univ. Grenoble 1/CNRS, LPMMC UMR 5493, maison des magistères, 38042 Grenoble, France*
[b] *SPSMS, UMR-E 9001 CEA/UJF-Grenoble 1, INAC, 38054 Grenoble, France*
[c] *Departments of Physics, Yale University, New Haven, CT 06520, USA*
[d] *Univ. Bordeaux, LOMA, UMR 5798, 33400 Talence, France*
[e] *CNRS, LOMA, UMR 5798, 33400 Talence, France*

ARTICLE INFO

Article history:
Available online 23 April 2012

Keywords:
Polaron
Quantum dot
Nano-electromechanical system

Mots-clés :
Polaron
Boîte quantique
Système nano-électromécanique

ABSTRACT

We investigate the electronic transport through a suspended carbon-nanotube quantum dot. In the presence of a magnetic field perpendicular to the nanotube and a nearby metallic gate, two forces act on the electrons: the Laplace and the electrostatic force. They both induce coupling between the electrons and the mechanical transverse oscillation modes. We find that the difference between the two mechanisms appears in the cotunneling current.

RÉSUMÉ

Nous étudions le transport électronique à travers un point quantique formé avec un nanotube de carbone suspendu. En présence d'un champ magnétique perpendiculaire au nanotube et d'une grille métallique, deux forces agissent sur les électrons : la force de Laplace et la force électrostatique. Elles induisent toutes les deux un couplage entre les électrons et les modes d'oscillations mécaniques transverses. Nous trouvons qu'une différence entre les deux mécanismes de couplage se manifeste à des ordres supérieurs dans le courant tunnel.

1. Introduction

Displacements of conducting nano-mechanical systems are conveniently registered by the electron transport measurements. The electron transport is sensitive to the mechanical motion mostly due to the electrostatic interaction, which allowed one to detect, e.g. the motion of tiny single systems, like C_{60} molecules [1] or carbon nanotubes [2]. The latter are particularly promising systems for many applications. High mechanical quality factors of the order of 10^5 have been reported for suspended carbon-nanotube oscillators [3]. At the same time, strong mechanical coupling to electronic transport,

* Corresponding author at: Laboratoire d'Ondes et Matière d'Aquitaine, Univ. Bordeaux and CNRS, UMR 5798, 351 cours de la Libération, 33400 Talence, France.
E-mail address: Fabio.Pistolesi@u-bordeaux1.fr (F. Pistolesi).

1631-0705/$ – see front matter
http://dx.doi.org/10.1016/j.crhy.2012.03.001

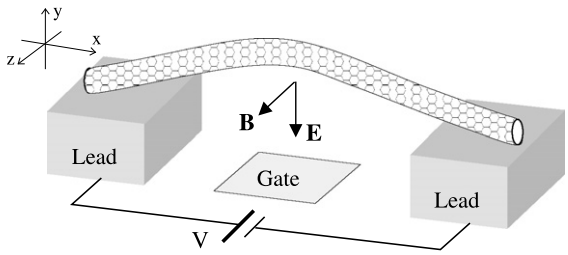

Fig. 1. Schematic picture of the system: a voltage biased suspended carbon nanotube in presence of a transverse magnetic field $\boldsymbol{B}$ and of a transverse electric field $\boldsymbol{E}$ created by applying a gate voltage.

both in the bending [4,5] and breathing modes [6,7], have also been demonstrated. The effect of the electrostatic coupling to the mechanical oscillations (also known as *polaronic* coupling) on transport has been investigated by several authors from the theoretical point of view [8–15]. A suppression of the current at low bias voltage, known as Franck–Condon blockade, has been predicted [12,16] and observed [7] in the quantum regime, for high frequency molecular oscillators. Similar effects in the classical limit (low frequency oscillators) have also been discussed [17–22].

Much less investigated is the effect of magnetic field, see Fig. 1, on the coupling between electronic transport and mechanical oscillations (called *magneto-elastic* coupling hereafter). This coupling is at the origin of the magnetomotive effect, which has been used to activate and detect the classical motion of micro- and nano-mechanical resonators since a long time. However its manifestation in the quantum regime has been addressed only recently for a suspended carbon nanotube forming a quantum dot [23–26]. A particularly appealing interpretation of the magnetoresistance in this system has been put forward in Ref. [23]: In the tunneling limit the electrons traversing the nanotube interfere over the different paths generated by its zero-point oscillations. The reduction of the current can then be seen as a joint manifestation of the Aharonov–Bohm effect and the quantum fluctuations of the mechanical degree of freedom. In the resonant case the magnetoresistance has been calculated as an expansion up to the second order in the small electromechanical coupling. It has been found that multiple interferences increase the size of the effect parametrically [25].

In any realistic device both the electrostatic and magnetic effects are present. The aim of the present article is to discuss the interplay of these two interactions. Specifically the system considered is shown schematically in Fig. 1. It consists in a suspended carbon nanotube forming a quantum dot contacted electrically to two external leads. We focus on the coupling of the fundamental bending mode of the nanotube to the electronic transport in presence of both a strong magnetic field perpendicular to the nanotube and a metallic gate. They induce a magneto-elastic and a polaronic coupling, respectively. We consider a high-temperature regime when electron tunneling events between the leads can be described in terms of rate equations [27,28]. On the other hand, the mechanical mode is in the low-temperature limit and, for simplicity, we will further assume that its coupling to the environment is sufficiently strong to keep the oscillator in equilibrium.

The theory that is formulated in the reminder of the paper allows to explore the purely magnetic problem outside the limits of previous works [23–25], by investigating transport at bias voltages larger than the oscillator's energy quantum. The same approach is then used to study the interplay between the magneto-elastic and polaronic couplings. In the sequential tunneling regime, we find that the current depends on a single coupling constant which is the root mean square of the polaronic and magneto-elastic coupling constants, respectively. The presence of a magnetic field at this order thus only renormalizes the effective interaction and introduces a Zeeman splitting of the electronic levels.

The difference between the two interactions appears in the cotunneling regime (when electrons tunnel directly between the leads through virtual states in the dot). When the single energy level in the dot is close or in the conducting window between the left and right chemical potential of the leads (resonant transport) cotunneling events induce a small correction to the current. However, they can dominate transport away from resonance. It is thus in that regime that the difference between the polaronic and magneto-elastic couplings becomes clear-cut and could be detected experimentally.

The article is organized as follows. Section 2 is dedicated to the microscopic derivation of the model Hamiltonian used in the reminder of the paper. Section 3 introduces the formalism used to tackle the problem. In Section 4 we discuss the behavior of the current as obtained in the sequential tunneling approximation and the consequences of the Zeeman splitting. Section 5 considers the contribution of the cotunneling events, discussing in particular the difference between the polaronic and magneto-elastic couplings. Section 6 gives our conclusions. Part of the material is presented in the appendices.

2. Model Hamiltonian

We derive the Hamiltonian for a suspended nanowire weakly electronically coupled to leads in presence of polaronic and magneto-elastic effects in Sections 2.1–2.3, see Eqs. (40), (41). We estimate the amplitudes of these effects for a quantum dot formed with a suspended carbon nanotube in Section 2.4.

2.1. Magneto-elastic coupling

In this subsection we present a detailed microscopic derivation of the magneto-elastic interaction. It extends the model proposed in the previous works [23,25].

2.1.1. Electron in a vibrating nanowire

The Hamiltonian that describes an electron propagating in a ballistic, suspended nanowire in presence of a transverse magnetic field (units with $\hbar = k_B = 1$ are used throughout the paper) is

$$\mathcal{H} = \frac{1}{2m}\big(\boldsymbol{p} + e\boldsymbol{A}(\boldsymbol{r})\big)^2 + V\big(x, y - u(x), z\big) + H_{\text{string}} \tag{1}$$

Here, $\boldsymbol{p} = (p_x, p_y, p_z)$ and $\boldsymbol{r} = (x, y, z)$ are the momentum and position of the electron of mass m and charge $-e$, $\boldsymbol{A} = (-By, 0, 0)$ is the vector potential associated with the magnetic field $\boldsymbol{B} = (0, 0, B)$. The potential

$$V\big(x, y - u(x), z\big) = V_b(x) + V_{\text{conf}}\big(y - u(x), z\big) \tag{2}$$

contains two terms. The first one describes the tunnel barriers between the nanowire and the leads,

$$V_b(x) = V_l\delta(x) + V_r\delta(x - L) \tag{3}$$

where L is the nanowire's length. The second one is the confining potential V_{conf} inside the nanowire, it depends on the deflection $u(x)$ of the nanowire along the y-direction.

The elastic bending of the nanowire in the (x, y)-plane is described within the elastic string theory [29] with the term

$$H_{\text{string}} = \int_0^L \mathrm{d}s \left[\frac{\pi^2}{2\rho} + \frac{EI}{2}\left(\frac{\partial^2 u}{\partial s^2}\right)^2\right] \tag{4}$$

where ρ is the mass per unit length of the string, E is its elastic Young's modulus, and I is its area momentum of inertia, the deflection field and momentum density operators of the string are conjugated $[u(s), \pi(s')] = i\delta(s - s')$. For a doubly clamped nanowire, the boundary conditions are $u(s) = \partial_s u(s) = 0$ at $s = 0, L$.

The classical mechanical eigenmodes of the nanowire are characterized by a frequency ω_n – the lowest mode has frequency $\omega_0 \approx 22.4(EI/\rho L^4)^{1/2}$ – and displacement field $f_n(s)$ (integer $n \geqslant 0$) with normalization $(1/L)\int_0^L \mathrm{d}s\, f_n(s)^2 = 1$. Decomposing the deflection field operator onto these modes,

$$u(s) = \sum_n X_n f_n(s) \tag{5}$$

the Hamiltonian (4) then becomes:

$$H_{\text{string}} = \sum_n \left(\frac{P_n^2}{2M} + \frac{M\omega_n^2 X_n^2}{2}\right) \tag{6}$$

where X_n and P_n are the effective positions and momenta of the modes, with conjugation relation $[X_n, P_m] = i\delta_{nm}$, and $M = \rho L$ is the mass of the nanowire.

We can reasonably expect that the confining potential enforces the replacement $y \to u(x)$ in Eq. (1), assuming that the nanowire stands along a line with $y = 0$ in classical equilibrium. The one-dimensional propagation of the electron and its coupling to the vibrations would then be described by

$$\mathcal{H} \approx \frac{1}{2m}\big[p_x - eBu(x)\big]^2 + V_b(x) + H_{\text{string}} \tag{7}$$

A unitary transformation $\mathcal{H} \to e^{i\mathcal{S}}\mathcal{H}e^{-i\mathcal{S}}$ where $\mathcal{S} = -eBU(x)$, with $\partial_x U(x) = u(x)$ would then yield:

$$\mathcal{H} = \mathcal{H}_0 + \sum_n \left(\frac{[P_n + eBF_n(x)]^2}{2M} + \frac{M\omega_n^2 X_n^2}{2}\right) \tag{8}$$

where $\mathcal{H}_0 = p_x^2/(2m) + V_b(x)$ and $F_n(x) = \int^x \mathrm{d}s\, f_n(s)$, which will be the starting point of the next section.

Appendix A is devoted to a rigorous derivation of Eq. (8) starting from Eq. (1) and taking into account the transverse spreading of the electron's wavefunction in the nanowire.

2.1.2. Single-level regime

Here we simplify further the Hamiltonian (8) in the regime of a single resonant electronic level in the nanowire.

Indeed, the term $\mathcal{H}_0$ in Eq. (8) describes an electron propagating through a double-barrier system. For strong tunnel barriers, quasi-localized states are formed in the central region. Due to the coupling with the leads in the outer regions, they decay with a lifetime $1/\Gamma$. Assuming a large energy level spacing $\Delta \gg \Gamma$ between the quasi-localized states, we can focus on a single level with energy ε_d in the central part of the nanowire, provided that the chemical potential μ in the leads is also close to the single-level energy, $|\mu - \varepsilon_d| \ll \Delta$.

In this regime, the single-particle Hamiltonian $\mathcal{H}_0$ entering Eq. (8) can be written equivalently

$$\mathcal{H}_0 = \mathcal{H}_L + \mathcal{H}_d + \mathcal{H}_T \tag{9}$$

where

$$\mathcal{H}_L = \sum_{k,\nu} \varepsilon_k c^\dagger_{k\nu} c_{k\nu} \tag{10}$$

$$\mathcal{H}_d = \varepsilon_d d^\dagger d \tag{11}$$

$$\mathcal{H}_T = \sum_{k,\nu} \left(t_\nu c^\dagger_{k\nu} d + \text{h.c.} \right) \tag{12}$$

describe the leads, the dot, and their tunnel coupling, respectively. Here, $c_{k\nu}$ ($\nu = l, r$) are the annihilation operators for the electron propagating states in the left (l) and right (r) leads, labeled with momenta k, and energies $\varepsilon_k = k^2/2m$; d is the annihilation operator in a single-level state of the nanotube, with energy $\varepsilon_d = \pi^2 p^2/(2mL^2)$ (p is a strictly positive integer). The wavefunction associated with this level is $\sqrt{2/L}\sin(\pi px/L)$. The tunnel coupling between this state and the continuum of states in the leads is accounted with the tunnel matrix elements t_ν. Each lead contributes to the single-level energy broadening $\Gamma_\nu = 2\pi N_\nu |t_\nu|^2$, respectively, where N_ν are the densities of states (per spin) at the Fermi level in the leads ($\Gamma = \Gamma_l + \Gamma_r$ is the total broadening). They can be related with the parameters in Eq. (3) through the relations $\Gamma_\nu = 2\pi^{-1}\Delta(\mu/V_\nu k_F)^2$ at $\nu = l, r$, where $\Delta \approx \pi^2 p/mL^2$ (at large p) and k_F is the Fermi wavevector.

We use the basis of electron states defined above to write the resolution of the identity (for the single-particle problem considered here) as $\mathbb{1} = n_l + n_r + n_d$, where $n_\nu = \sum_k c^\dagger_{k\nu} c_{k\nu}$ and $n_d = d^\dagger d$ count whether the electron is in the left lead, right lead, or the dot, respectively. Inserting it on the right and left sides of Eq. (8) and also assuming that $\Delta \gg \omega_n$ for the relevant oscillator's eigenmodes, we find that the Hamiltonian coupling the states with energies close to the Fermi level reads

$$\mathcal{H} = \mathcal{H}_0 + \sum_n \left(M\omega_n^2 X_n^2/2 + K_{nl} n_l + K_{nr} n_r + K_{nd} n_d \right) \tag{13}$$

with

$$K_{nl} = \frac{[P_n - eBF_n(0)]^2}{2M} \tag{14a}$$

$$K_{nr} = \frac{[P_n - eBF_n(L)]^2}{2M} \tag{14b}$$

$$K_{nd} = \frac{[P_n - eB\langle F_n\rangle]^2}{2M} + \frac{e^2B^2}{2M}\left(\langle F_n^2\rangle - \langle F_n\rangle^2 \right) \tag{14c}$$

and

$$\langle F_n^\alpha \rangle = \frac{2}{L}\int_0^L \mathrm{d}x \, \sin^2\left(\frac{\pi px}{L}\right) F_n^\alpha(x) \tag{15}$$

for $\alpha = 1, 2$.

In order to eliminate the B-dependent terms in Eqs. (14), we perform another unitary transformation $\mathcal{H} \to e^{i\mathcal{S}'}\mathcal{H}e^{-i\mathcal{S}'}$, with

$$\mathcal{S}' = -eB\sum_n \left[n_l F_n(0) + n_r F_n(L) + \langle F_n\rangle n_d \right] X_n \tag{16}$$

and we find

$$\mathcal{H} = H_{\text{string}} + \mathcal{H}_L + \tilde{\mathcal{H}}_d + \tilde{\mathcal{H}}_T \tag{17}$$

Here,

$$\tilde{\mathcal{H}}_d = \tilde{\varepsilon}_d d^\dagger d \tag{18}$$

where

$$\tilde{\varepsilon}_d = \varepsilon_d + \frac{e^2B^2}{2M}\left(\langle F_n^2\rangle - \langle F_n\rangle^2\right) \tag{19}$$

includes a diamagnetic shift for the single level, and

$$\tilde{\mathcal{H}}_T = \sum_k \left\{ t_l \exp\left(ieB \sum_n X_n \left[\langle F_n\rangle - F(0)\right]\right) c_{kl}^\dagger d + \text{h.c.}\right\} + \sum_k \left\{ t_r \exp\left(ieB \sum_n X_n \left[\langle F_n\rangle - F(L)\right]\right) c_{kr}^\dagger d + \text{h.c.}\right\} \tag{20}$$

Introducing the bosonic annihilation operators b_n for the oscillator's modes (phonons), with $X_n = X_{n0}(b_n + b_n^\dagger)$ ($X_{n0} = 1/\sqrt{2M\omega_n}$ is the amplitude of zero-point motion in the eigenmode n), we write

$$H_{\text{string}} = \sum_n \omega_n b_n^\dagger b_n \tag{21}$$

We also notice that the eigenmodes of the doubly clamped nanotube have a definite parity and, thus, $F_n(L) - \langle F_n\rangle = (-)^n[\langle F_n\rangle - F_n(0)]$. We then rewrite Eq. (20) as

$$\tilde{\mathcal{H}}_T = \sum_{k\nu} \left\{ t_\nu \exp\left[i \sum_n \left(b_n + b_n^\dagger\right)\phi_{\nu n}\right] c_{k\nu}^\dagger d + \text{h.c.}\right\} \tag{22}$$

where $\phi_{ln} = (-)^{n+1}\phi_{rn} = \phi_n$ and

$$\phi_n = \frac{4\pi B X_{n0} L}{\Phi_0} \int_0^L \frac{\mathrm{d}x}{L} \sin\left(\frac{\pi p x}{L}\right)^2 \int_0^x \frac{\mathrm{d}s}{L} f_n(s) \tag{23}$$

is the effective magnetic flux, in units of the flux quantum $\Phi_0 = 2\pi/e$, that characterizes the coupling between the electron and the eigenmode n of the oscillator. Integration by parts allows simplifying Eq. (23) into:

$$\phi_n = \frac{\pi B X_{n0} L}{\Phi_0} \int_0^L \frac{\mathrm{d}x}{L} f_n(x) \tag{24}$$

at even n, while a similar formula with an extra factor $1 - 2x/L + \sin(2\pi px/L)/(\pi p)$ in the integrand holds at odd n.

Eq. (17) together with (22) is the final result of this section. It generalizes the Hamiltonian derived in Ref. [23] that only considered the lowest eigenmode. [Note that different conditions are obtained to justify its validity (see Appendix A) and that the phase (24) is smaller by a factor 2π here.] The phase (23) was interpreted there as an Aharonov–Bohm phase picked by the electrons when they cross the tunnel barriers, and which depends on the deflection of the nanowire.

2.2. Polaron coupling

In this subsection we generalize the model to include the electrostatic coupling and the presence of the spin degree of freedom. We begin by adding an electrostatic contribution to the Hamiltonian (22) [30]

$$H_C = \frac{e^2N^2}{2C_g[u(s)]} - eV_gN \tag{25}$$

where C_g is the gate capacitance (we took a current with typical amplitude $e\omega_n$ for the last estimate are negligible with respect to the gate capacitance), V_g is the gate voltage, and N is the operator for the total number of electrons on the dot. Since we assume that only a single level contributes to transport, it is possible to write $N = N_0 + n_d$, where $N_0 \approx C_gV_g/e$ is the number of the excess electrons in the filled levels, and n_d is the number of electrons in the relevant level. For small displacement of the oscillator we can express $C_g[u(s)]$ in terms of X_n:

$$C_g\left[u(s)\right] = C_g[0]\left(1 - \sum_n a_n X_n\right) \tag{26}$$

where

$$a_n = -\int_0^L \frac{\mathrm{d}s}{L} \frac{1}{C_g[0]} \frac{\partial C_g}{\partial u}[0] f_n(s) \tag{27}$$

Substituting the expansion (26) into (25) one obtains (apart from a constant term):

$$H_C = \frac{U_\infty}{2}\sum_n a_n X_n + U_\infty n_{d\uparrow} n_{d\downarrow} + (\delta\varepsilon - eV_g)\, n_d + H_{\rm pol} \tag{28}$$

where $n_{d\sigma} = d_\sigma^\dagger d_\sigma$, $n_d = n_{d\uparrow} + n_{d\downarrow}$, $U_\infty = e^2/C_g[0]$, $\delta\varepsilon = U_\infty(2N_0+1)/2$, and

$$H_{\rm pol} = \sum_n \lambda_n \omega_n \big(b_n + b_n^\dagger\big) n_d \tag{29}$$

with $\lambda_n = a_n \delta\varepsilon X_{n0}/\omega_n$. The first term of Eq. (28) gives a shift in the equilibrium position of the oscillator and can be discarded. The second term gives the intradot Coulomb repulsion. We will assume that U_∞ is the largest energy scale of the problem, allowing to neglect the contribution of the double occupancy state [the term proportional to U_∞ times X_n can be neglected for the same reason and it is not shown in Eq. (28)]. The third term can be included in the definition of $\tilde{\varepsilon}_d$ since it gives only a renormalization of the energy of the level. The last term, defined in Eq. (29), is the seeked polaronic coupling, which models the interaction between the oscillation modes and the charge fluctuations in the dot.

The expression for the polaronic coupling constant can be calculated by using a model of a distributed capacitance [30,31]:

$$C_g\big[u(s)\big] = \int_0^L {\rm d}s\, \frac{2\pi\epsilon_0}{\operatorname{arccosh}([(h-u(s)]/R_\perp)} \tag{30}$$

where h is the distance of the nanotube from the substrate, $R_\perp$ its radius, and ϵ_0 is the vacuum permittivity. Substituting Eq. (30) in the definition of λ_n and calculating the integral for $u = 0$ and $R_\perp \ll h$ one obtains:

$$\lambda_n \approx \frac{eC_g[0]|V_g|}{2\pi\epsilon_0 hL}\,\frac{X_{n0}}{\omega_n}\int_0^L \frac{{\rm d}s}{L} f_n(s) \tag{31}$$

for $C_g[0]V_g \gg e$.

Including the electrostatic coupling and the spin degrees of freedom to the Hamiltonian (22) we obtain:

$$H = H_{\rm string} + H_L + H_d + H_T \tag{32}$$

where the term $H_{\rm string}$ remains unchanged, see Eq. (21). The inclusion of the spin and the chemical potentials gives instead

$$H_L = \sum_{\nu,k,\sigma} \xi_{\nu k} c_{\nu k\sigma}^\dagger c_{\nu k\sigma} \tag{33}$$

where $c_{\nu k\sigma}$ is the annihilation operator for a state with momentum k and spin $\sigma = \uparrow, \downarrow$ in lead $\nu = l, r$, $\xi_{\nu k} = \varepsilon_k - \mu_\nu$, and the difference of the chemical potentials $\mu_l - \mu_r = eV$ is related to the bias voltage V of the junction. The dot local term modified by the presence of the magnetic field and the electrostatic interaction reads:

$$H_d = \sum_\sigma \varepsilon_{d\sigma} d_\sigma^\dagger d_\sigma + U_\infty n_{d\uparrow} n_{d\downarrow} + H_{\rm pol} \tag{34}$$

Here $\varepsilon_{d\sigma} = \tilde{\varepsilon}_d + \delta\varepsilon + \sigma\mu_B B$ ($\sigma = +$ for $\uparrow$, $\sigma = -$ for $\downarrow$), and μ_B is the Bohr magneton. Note that we included the Zeeman splitting in the spectrum of the dot, but we don't need to include it in the lead spectrum, since the density of states of metallic leads can be considered as constant at the Fermi energy. The last term describes tunneling and generalizes the one entering Eq. (22) to take into account the spin:

$$H_T = \sum_{\nu,k,\sigma}\left\{ t_\nu \exp\left[i\sum_n \big(b_n + b_n^\dagger\big)\phi_{\nu n}\right] c_{\nu k\sigma}^\dagger d_\sigma + {\rm h.c.}\right\} \tag{35}$$

In the absence of magneto-elastic coupling, the Hamiltonian (32) was introduced in Refs. [8,9] to describe transport through a quantum dot in presence of a local electron–phonon coupling and later studied by several authors [12,13,16,27,32,33].

2.3. Combined coupling constant

The expression for the Hamiltonian can be further manipulated in such a way that the dimensionless coupling constants ϕ_n and λ_n introduced in Sections 2.1 and 2.2, respectively, can be treated on the same footing.

For this purpose it is convenient to eliminate the linear polaron coupling in the Hamiltonian (34) by using the Lang–Firsov unitary transformation $H \to UHU^\dagger$:

$$U = e^{-\sum_n \lambda_n (b_n - b_n^\dagger)(n_{d\uparrow} + n_{d\downarrow})} \tag{36}$$

The transformation shifts the bosonic fields ($U b_n U^\dagger = b_n - \lambda_n n_d$) giving for $H_{\rm string} + H_d$:

$$H_d + H_{\rm string} \to \sum_n \omega_n b_n^\dagger b_n + \sum_\sigma \tilde{\varepsilon}_{d\sigma} n_{d\sigma} + \tilde{U}_\infty n_{d\uparrow} n_{d\downarrow} \tag{37}$$

with $\tilde{\varepsilon}_{d\sigma} = \varepsilon_{d\sigma} - \sum_n \lambda_n^2 \omega_n$ and $\tilde{U}_\infty = U_\infty - 2\sum_n \lambda_n^2 \omega_n$. Both the energy of the dot level and the effective interaction between two electrons on the dot are renormalized. Note that, for $U_\infty < 2\sum_n \lambda_n^2 \omega_n$, the effective interaction can become attractive [16,34]. Focusing our analysis to strong Coulomb repulsion regime we are not concerned by this possibility.

Using $U d_\sigma U^\dagger = d_\sigma e^{\sum_n \lambda_n (b_n - b_n^\dagger)}$ and Baker–Hausdorff formula, the tunneling term in Eq. (35) becomes

$$U\big(e^{i\sum_n (b_n + b_n^\dagger)\phi_{\nu n}} d_\sigma\big) U^\dagger = e^{-i\sum_n \lambda_n \phi_{\nu n}} e^{-2i\sum_n \lambda_n \phi_{\nu n} n_{d\bar{\sigma}}} \exp\left[\sum_n \big(\alpha_{\nu n} b_n - \alpha_{\nu n}^* b_n^\dagger\big)\right] d_\sigma \tag{38}$$

where $\bar{\sigma}$ indicates the spin projection opposite to σ. In Eq. (38) we have introduced the *complex* electron–phonon coupling constants:

$$\alpha_{\nu n} = \lambda_n + i\phi_{\nu n} \tag{39}$$

Let us first discuss the effect of the prefactor $\exp(-2i\sum_n \phi_{\nu n}\lambda_n n_{d\bar{\sigma}})$. Since we are considering the limit where double occupied states are not accessible, it is easy to show that this term gives always 1 when evaluated with d_σ on the three dot's basis states $\{|0\rangle, |\uparrow\rangle, |\downarrow\rangle\}$. We will thus drop it in the following. The phase factor $\exp(-\sum_n i\phi_{\nu n}\lambda_n)$ can be included in the definition of the tunneling amplitude t_ν.

Combining the above results, we finally obtain the Hamiltonian

$$H = \sum_n \omega_n b_n^\dagger b_n + \sum_{\nu,k,\sigma} \xi_{\nu k} c_{\nu k\sigma}^\dagger c_{\nu k\sigma} + \sum_\sigma \tilde{\varepsilon}_{d\sigma} n_{d\sigma} + \tilde{U}_\infty n_{d\uparrow} n_{d\downarrow} + \tilde{H}_T \tag{40}$$

with the tunneling Hamiltonian:

$$\tilde{H}_T = \sum_{\nu,k,\sigma} \left\{ t_\nu \exp\left[\sum_n \big(\alpha_{\nu n} b_n - \alpha_{\nu n}^* b_n^\dagger\big)\right] c_{\nu k\sigma}^\dagger d_\sigma + \text{h.c.} \right\} \tag{41}$$

In Eq. (41) the polaronic and magneto-elastic couplings enter on the same footing through constants $\alpha_{\nu n}$, see Eq. (39).

2.4. Discussion

Remarkably, the ratio between the magneto-elastic and polaronic coupling constants, cf. Eqs. (24) and (31), is independent of the length of the nanotube. A crude estimate shows that, for the fundamental bending mode, $\phi_0/\lambda_0 \sim \sqrt{m/m^*}(e/C_g|V_g|)Bha_B/\Phi_0$, where a_B is the Bohr radius and m^* is the nucleon mass. (To get it we used $\rho \sim m^*/a_B$, $I \sim R_\perp^4 \sim a_B^4$, and $E \sim Ry/a_B^4$, where Ry is the Rydberg energy.) In the ratio ϕ_0/λ_0, the smallness of m/m^* is compensated by the largeness of h/a_B. Thus, magneto-elastic and polaronic coupling constants of the same order of magnitude could be realized, while being tunable independently through the magnetic field and gate voltage. It is thus interesting to investigate their interplay in the transport properties of the device.

Let us now estimate the coupling constants quantitatively. Assuming a linear mass density ρ of the order of 10^{-15} kg/m, corresponding to six carbon atoms/Å, and a length L of 1 μm, we find that the typical mass of a single-wall carbon nanotube is 10^{-21} kg. The zero-point motion X_{n0} for a mode of frequency $\omega_n/2\pi = 500$ MHz is 4 pm. For $B = 40T$, Eq. (24) yields $\phi_0 \approx 0.1$ for the fundamental bending mode [for which $\int_0^L (\mathrm{d}s/L) f_0(s) \simeq 0.83$], while, for $h = 200$ nm and $C_g V_g = 5e$, one finds from Eq. (31) that $\lambda_0 \approx 0.1$. The magnitude of the magneto-elastic and polaronic effects is thus the same for these parameters.

It is probably useful to point out that the current dependence generated by the strong magnetic field discussed in this paper and in previous works [23–25] is totally unrelated to the Aharonov–Bohm effect discussed in the literature in several papers (see Ref. [35] for a review). The effect discussed there is due to the interference of the electrons in the Aharonov–Bohm loops generated by the carbon crystallographic structure. The presence of phonon modes is not required for this effect to be present, while it is crucial for the magnetoresistance discussed here. It should be also noted that the two contributions are of course present at the same time in a realistic description of the carbon nanotube, but the two effects can be distinguished experimentally since they have totally different thermal and voltage dependences [25].

Concerning the model for the description of the nanotube deformation, in this paper we assumed that the standard theory of elastic continuous media applies. This should be correct, at least for not too short nanotubes, where an atomic description becomes necessary. We only considered the case of a rigid rod with doubly clamped boundary conditions. It is well known that it is possible to observe a crossover from this regime to the regime of tense string [2]. The effect of a residual stress on the string can be taken into account by modifying the Hamiltonian (4) [29]. The structure of Eq. (22)

remains valid in this case. The effect of the tension modifies only the profile function $f_n(s)$ entering Eq. (23) for the eigenmodes. The elongation of the nanotube induced by the external gate and magnetic field, with typical amplitude $\sim\lambda_n X_{n0}$ and $\phi_n X_{n0}$ respectively (we took a current with typical amplitude $e\omega_n$ for the last estimate), also generates an internal stress. The nonlinear effects induced by this stress are safely neglected when these amplitudes do not exceed $R_\perp$ [29], which is the case for the parameters given above.

The amplitudes of the effective phases in the tunneling part of Eq. (22) only coincide for symmetric boundary conditions. For instance, in the case of a nanotube that is clamped on one side and *hanging* on the other side, no specific relation would exist between the phases in the left and right terms.

Surprisingly the Hamiltonian (40)–(41) with $\lambda_n = 0$ has been already introduced before (in spinless case) for a quite different problem. Imam et al. [36] considered resonant tunneling in presence of an electromagnetic environment associated with the fluctuations of the bias voltage, and described by a bath of phonon modes. Nevertheless, the effect of the environment on the conductance was only addressed at large bias voltage or far from the resonance in that work. Moreover in this paper we address the interplay of the magnetic and polaronic coupling, that was not present there.

3. Formalism

Our aim is to derive the current–voltage characteristics for the problem described with Hamiltonian (40), (41). (Note that tildes that appear there will be omitted from now on.) Here we present the general approach that will be used in the next sections.

The problem at hand is a generalization of the well studied polaron problem. It has not been solved exactly yet, to the best of our knowledge. Nevertheless, it is possible to obtain approximate results in different regimes. When the coupling constant is small, a perturbative expansion is possible; it has been performed both for the polaronic [15] and the magneto-elastic cases [25]. In principle the method used in those previous publications can be extended to investigate the case when both couplings are present. However it works only when the predicted effects are small and we will not use it in this article. Alternatively, the dynamics of a single electron in the presence of the phonon bath can be obtained [8,36]. However, the results obtained for the phonon-assisted resonant tunneling can only be applied far from the resonance, when effects associated with the Fermi sea in the leads can be neglected. Another tractable limit is the case of high-temperature incoherent tunneling limit ($T \gg \Gamma$), which has been discussed in Ref. [27] for the polaron problem and does not require that the electron–phonon coupling is perturbative. Here, we generalize this approach to describe the effect of the interplay of the two couplings.

In this incoherent regime the electronic environment at temperature T has the time to suppress the coherence of the quantum evolution between tunneling events. The equations of motion for the off-diagonal elements of the density matrix in the basis of the eigenvectors of $H_0 = H - H_T$ decouple from those for the diagonal elements. It is then possible to obtain the equations of motion for the diagonal elements (*i.e.* the occupation probabilities) alone.

The rates can be obtained by standard perturbation theory. The time evolution of any eigenstate $|i\rangle$ of H_0 can be written in terms of the resolvent:

$$|i\rangle(t) = \int \frac{\mathrm{d}E}{2\pi} \frac{e^{-iEt}}{E - H_0 - H_T + i\eta} |i\rangle \tag{42}$$

The probability that the system is in another state $|f\rangle$ after a time t is

$$P_{if} = \left| \int \frac{\mathrm{d}E}{2\pi} e^{-iEt} \langle f | G^0(E) + G^0(E) T(E) G^0(E) | i \rangle \right|^2 \tag{43}$$

where $T(E) = H_T + G^0(E) H_T G^0(E) + \cdots$ is the T-matrix and $G^0(E) = (E - H_0 + i\eta)^{-1}$ is the free retarded propagator. Neglecting the E dependence of $T(E)$ in Eq. (43) gives the standard Fermi golden rule with $T(E_i)$ replacing H_T, that is, $P_{if} = tW_{if}$ with

$$W_{if} = 2\pi \left| T_{if}(E_i) \right|^2 \delta(E_i - E_f) \tag{44}$$

and E_i the eigenvalue of H_0 related to the state i. By inserting the resolution of the identity in terms of the eigenstates of H_0, one can then write for the first two orders:

$$\left| T_{if}(E_i) \right|^2 = \left| (H_T)_{if} + \sum_n \frac{(H_T)_{in}(H_T)_{nf}}{E_i - E_n} \right|^2 \tag{45}$$

These two terms give the tunneling and cotunneling contributions to the transition rate, respectively. We will investigate the effect of the tunneling term in Section 4 and then the corrections given by the cotunneling terms in Section 5. A comment is at order. The expression (44) holds if the frequency dependence of $T(\omega)$ is sufficiently smooth. This is not true if one intermediate state has the same energy as the final state. The problem has been discussed in Ref. [27] and it requires a proper renormalization of the divergences of the integrals appearing in the calculation of the transition rates. The regularization for the transition rates associated with cotunneling processes is done in Appendix B.

The system state is thus completely described by the probability of being in one of the eigenstates of H_0. We will assume that the lead remains in thermal equilibrium during the evolution, thus the only relevant degrees of freedom left are the dot and oscillator degrees of freedom. In the following we will focus on a single phononic mode, for which we define ω the resonance frequency, ϕ the magneto-elastic coupling, and λ the polaronic coupling. In order to fully describe the system we finally define the probability $p_{sn}(t)$ that the dot is in one of the three available states ($|s\rangle = |0\rangle, |\downarrow\rangle, |\uparrow\rangle$) and the oscillator in the phonon state n ($|n\rangle = b^{\dagger n}|0\rangle/\sqrt{n!}$). The rate equations read:

$$\frac{\mathrm{d}p_{sn}}{\mathrm{d}t} = \sum_{m=0}^{\infty} \sum_{s'=0,\uparrow,\downarrow} [W_{s'm,sn} p_{s'm} - W_{sn,s'm} p_{sn}] - \frac{1}{\tau}\left(p_{sn} - P_n^{(\mathrm{eq})} \sum_{m=0}^{\infty} p_{sm}\right) \tag{46}$$

Here $W_{sn,s'm}$ is the transition rate from the electronic dot state s and phonon state n to another configuration (s', m). Following Ref. [27], a phenomenological relaxation term has been introduced in Eq. (46) to describe the coupling of the oscillator with the non-electronic environment at the origin of an intrinsic finite quality factor $Q^{-1} = \omega\tau/2\pi$ for the oscillator. The function $P_n^{(\mathrm{eq})}$ gives the equilibrium phonon distribution function:

$$P_n^{(\mathrm{eq})} = \left(1 - e^{-\omega/T}\right) e^{-n\omega/T} \tag{47}$$

Given the rates, Eq. (46) can be solved; the average current is then obtained from the stationary solution for the probabilities. In the next two sections, we discuss the result for the current at the sequential (Section 4) and cotunneling (Section 5) orders.

4. Sequential tunneling regime

The sequential tunneling regime corresponds to keeping only the lowest order term in the expansion (45) that determines the transition rates. In this regime we find that the current–voltage characteristics depends on a single coupling constant which does not allow to distinguish the polaronic and magneto-elastic effect from each other.

4.1. General formula

The explicit form of the transition rates in the sequential tunneling limit reads:

$$W_{sn,s'm} = \sum_{\nu=l,r} W^{(\nu)}_{sn,s'm} \tag{48}$$

with

$$W^{(\nu)}_{sn,s'm} = 2\pi \sum_{i_\nu, f_\nu} P^{(\mathrm{eq})}(i_\nu) \left|\langle f_\nu, s', m | H_T | i_\nu, s, n\rangle\right|^2 \delta\left(E_{f_\nu} - E_{i_\nu} + \varepsilon_{ds'} - \varepsilon_{ds} + \omega[m-n]\right) \tag{49}$$

Here i_ν and f_ν are initial and final fermionic states in lead ν, with energies E_{i_ν} and E_{f_ν}, $P^{(\mathrm{eq})}(i_\nu)$ is the equilibrium distribution of state i_ν, and for convenience we introduced $\varepsilon_{d0} \equiv 0$. The non-vanishing rates take the form:

$$W^{(\nu)}_{0n,\sigma m} = \Gamma_\nu \left|M^{(\nu)}_{nm}\right|^2 n_\nu\left(\varepsilon_{d\sigma} + \omega[m-n]\right) \tag{50}$$

$$W^{(\nu)}_{\sigma m,0n} = \Gamma_\nu \left|M^{(\nu)}_{nm}\right|^2 \left[1 - n_\nu\left(\varepsilon_{d\sigma} + \omega[m-n]\right)\right] \tag{51}$$

where $n_\nu(\varepsilon) = 1/[e^{(\varepsilon-\mu_\nu)/T} + 1]^{-1}$ is the Fermi distribution in lead ν, $M^{(\nu)}_{nm} = \langle n | e^{\alpha_\nu b - \alpha_\nu^* b^\dagger} | m\rangle$, and we recall that $\Gamma_\nu = 2\pi |t_\nu|^2 N_\nu$.

The absolute value of the matrix element $M^{(\nu)}_{nm}$ depends only on $|\alpha_\nu| \equiv \alpha$, where

$$\alpha = \sqrt{\lambda^2 + \phi^2} \tag{52}$$

is the r.m.s. of the polaronic and magneto-elastic coupling constants. This can be readily shown by absorbing the phase of α_ν in the operators b and $b^\dagger$ appearing in the definition of $M^{(\nu)}_{nm}$. This is a surprising result, which holds only at this sequential order in the tunneling expansion. For instance, it was shown in Ref. [25] that there are qualitative differences between the magneto-elastic and the polaronic problems: at resonance, the maximum current depends on the asymmetry of the electronic coupling between the dot and the leads in the first case and does not in the second case. It is thus clear that to higher order differences have to appear. Technically this means that the current should depend also on the phase of the coupling α_ν, as we will find at the cotunneling level in Section 5.

In the reminder of this section we will study the evolution of the current–voltage characteristics as a function of the magnetic field. For simplicity we assume that the relaxation time introduced in Eq. (46) is shorter than the inverse of the typical tunneling rate, so that the distribution function can be written:

$$p_{sn} = P_s P_n^{(\mathrm{eq})} \tag{53}$$

The rate equation (46) for the stationary solution ($\mathrm{d}p_{sn}/\mathrm{d}t = 0$) can then be cast in the form $\mathbf{WP} = 0$, where $\mathbf{P} = (P_0, P_\uparrow, P_\downarrow)$ (with the normalization condition $P_0 + P_\uparrow + P_\downarrow = 1$),

$$\mathbf{W} = \sum_{\nu=l,r} \begin{pmatrix} -[W_{0\uparrow}^{(\nu)} + W_{0\downarrow}^{(\nu)}] & W_{\uparrow 0}^{(\nu)} & W_{\downarrow 0}^{(\nu)} \\ W_{0\uparrow}^{(\nu)} & -W_{\uparrow 0}^{(\nu)} & 0 \\ W_{0\downarrow}^{(\nu)} & 0 & -W_{\downarrow 0}^{(\nu)} \end{pmatrix} \tag{54}$$

and we define the *reduced* transition rates:

$$W_{ss'}^{(\nu)} = \sum_{n,m} P_n^{(\mathrm{eq})} W_{sn,s'm}^{(\nu)} \tag{55}$$

By performing the sum over the phonon states the rate takes a form similar to the non-interacting case: [12] $W_{0\sigma}^{(\nu)} = \Gamma_\nu \tilde{n}_\nu(\varepsilon_{d\sigma})$ and $W_{\sigma 0}^{(\nu)} = W_{0\sigma}^{(\nu)} e^{(\varepsilon_{d\sigma} - \mu_\nu)/T}$ with

$$\tilde{n}_\nu(\varepsilon) = \int \mathrm{d}E\, \mathcal{P}(E) n_\nu(\varepsilon + E) \tag{56}$$

Here the function $\mathcal{P}$ reads

$$\mathcal{P}(E) = \frac{1}{2\pi} \int \mathrm{d}t\, e^{iEt} \left\langle A_\nu(t) A_\nu^\dagger(0) \right\rangle \tag{57}$$

with $A_\nu(t) = e^{\alpha_\nu b(t) - \alpha_\nu^* b^\dagger(t)}$. In Fourier space, $\mathcal{P}(E)$ takes the form of a sum of delta functions centered at integers multiples of the oscillator frequency ω. In the limit $T \ll \omega$, on which we will focus hereafter, the oscillator is in the ground state and

$$\mathcal{P}(E) = \sum_{m=0}^{\infty} e^{-\alpha^2} \frac{\alpha^{2m}}{m!} \delta(E - m\omega) \tag{58}$$

The current, say for instance at the left lead, can be written in terms of the probabilities and the tunneling rates:

$$I = e \sum_{\sigma=\uparrow,\downarrow} \sum_{n,m=0}^{\infty} \left(W_{0n,\sigma m}^{(l)} p_{0n} - W_{\sigma m,0n}^{(l)} p_{\sigma m} \right) \tag{59}$$

In the case of interest here of the equilibrated oscillator one obtains:

$$I = \sum_{\sigma=\uparrow,\downarrow} (1 - P_{\bar{\sigma}}) I_\sigma \tag{60}$$

with the current for each spin-channel:

$$I_\sigma = e \Gamma_l \Gamma_r \frac{\tilde{n}_l(\varepsilon_{d\sigma}) \tilde{n}_r(\varepsilon_{d\sigma}) [e^{(\varepsilon_{d\sigma} - \mu_r)/T} - e^{(\varepsilon_{d\sigma} - \mu_l)/T}]}{\sum_\nu \Gamma_\nu \tilde{n}_\nu(\varepsilon_{d\sigma}) / n_\nu(\varepsilon_{d\sigma})} \tag{61}$$

and the stationary probabilities:

$$P_\sigma = \frac{\sum_{\nu,\nu'} \Gamma_\nu \Gamma_{\nu'} \tilde{n}_\nu(\varepsilon_{d\sigma}) \tilde{n}_{\nu'}(\varepsilon_{d\bar{\sigma}}) e^{(\varepsilon_{d\bar{\sigma}} - \mu_{\nu'})/T}}{\sum_{\nu,\nu'} \Gamma_\nu \Gamma_{\nu'} \tilde{n}_\nu(\varepsilon_{d\uparrow}) \tilde{n}_{\nu'}(\varepsilon_{d\downarrow}) [n_\nu^{-1}(\varepsilon_{d\uparrow}) n_{\nu'}^{-1}(\varepsilon_{d\downarrow}) - 1]} \tag{62}$$

with $P_0 = 1 - P_\uparrow - P_\downarrow$. Formula (60) for the sequential current has a simple interpretation: the current associated to the tunneling through one spin state and in absence of any correlation between the electrons is reduced by a factor which is just the probability of occupancy of the dot with opposite spin. Indeed, I_σ corresponds exactly to the sequential current for the spinless problem in presence of electron–phonon interaction.

From the previous expressions, we can obtain the linear conductance in the sequential tunneling regime:

$$G = G_0 \frac{\Gamma}{T} \frac{\tilde{n}(\varepsilon_{d\uparrow}) + \tilde{n}(\varepsilon_{d\downarrow})}{1 + 2e^{-(\varepsilon_d - \mu)/T} \cosh(\mu_B B/T)} \tag{63}$$

where $G_0 = e^2 \Gamma_l \Gamma_r / \Gamma^2$, $\varepsilon_d = (\varepsilon_{d\uparrow} + \varepsilon_{d\downarrow})/2$ and $\mu = (\mu_l + \mu_r)/2$. Eqs. (60)–(63) are the central result of this section. In the following we discuss the current in different regimes.

4.2. Linear conductance

The linear conductance generically displays a resonance as the energy ε_d of the discrete level in the dot is varied, e.g. with a gate voltage.

In the absence of electron–phonon interaction [37], the conductance is peaked around $\varepsilon_d - \mu \simeq (T/2)\log 2$, with width $\sim T$ and maximum height $G_{\max} = 2G_0(\Gamma/T)/(3+2\sqrt{2})$ at zero magnetic field. It is peaked around $\varepsilon_d - \mu \simeq \mu_B B$ (assuming $B > 0$), with width $\sim T$ and maximum height $G_{\max} = G_0\Gamma/(4T)$ at large magnetic field $\mu_B B \gg T$.

The main effect of electron–phonon interactions is to suppress the peak height: At low temperature ($T \ll \omega$), we find with help of Eqs. (56), (58) that the suppression factor is $e^{-\alpha^2}$ [8,12].

4.3. Nonlinear IV characteristics

In this section, we assume that the bias voltage is applied symmetrically, with $\mu_{l,r} = \mu \pm eV/2$.

In the absence of electron–phonon interaction and at zero magnetic field, resonance lines at $\varepsilon_d - \mu \simeq \pm eV/2$, with width $\sim T$, separate the regions where the current is blocked and those where it reaches a finite value $I = 2e\Gamma_l\Gamma_r/(\Gamma + \Gamma_l)$ or $I = -2e\Gamma_l\Gamma_r/(\Gamma + \Gamma_r)$, depending on the sign of the bias voltage [37]. At finite magnetic field, the regions where the current is blocked and those where down spins only can flow through the dot are separated by the lines $\varepsilon_d - \mu - \mu_B B \simeq \pm eV/2$. Inside the conducting regions it appears bands where an additional conduction channel opens for up spins. At $V > 0$ (respectively $V < 0$), these bands stand between the lines $\varepsilon_d - \mu - eV/2 = \pm\mu_B B$ ($\varepsilon_d - \mu + eV/2 = \pm\mu_B B$); the current reaches $I = e\Gamma_l\Gamma_r/\Gamma$ ($I = -e\Gamma_l\Gamma_r/\Gamma$) inside the bands. The contrast between the different lines in the gate and bias voltage dependence of the differential conductance, see Fig. 2, is readily explained by the amplitudes for the current found above between the lines.

The case of finite electron–phonon coupling and zero magnetic field was discussed in details in Refs. [12,16]. Note that Eq. (61) for the current simplifies into

$$I = 2e\Gamma_l\Gamma_r \frac{\tilde{n}_l(\varepsilon_d)\tilde{n}_l(\varepsilon_d)(e^{(\varepsilon_d-\mu_R)/k_BT} - e^{(\varepsilon_d-\mu_L)/k_BT})}{\sum_\nu \Gamma_\nu \tilde{n}_\nu(\varepsilon_d)(n_\nu^{-1}(\varepsilon_d)+1)} \tag{64}$$

The main features of the current are (i) the presence of inelastic lines (vibrational sidebands) at $\varepsilon_d - \mu + n\omega = \pm eV/2$ in the conducting regions and (ii) a suppression of the current at the low bias voltage (Franck–Condon blockade) when the electron–phonon coupling is large enough. Fig. 3 illustrates point (i) for intermediate electron–phonon coupling.

We can now understand the general features of the current when both the electron–phonon coupling and magnetic field are present. They look different depending on the ratio $\mu_B B/\omega$. When $\omega > \mu_B B$, the vibrational sidebands are split due to the removal of the spin degeneracy of the single level, see Fig. 4. When $\mu_B B > \omega$, vibrational sidebands are now present as replicas of the two main resonance lines, see Fig. 5.

In conclusion of this section, we found that the polaronic and magneto-elastic couplings cannot be distinguished in the sequential tunneling regime, apart from the removal of the spin degeneracy induced by the Zeeman effect. In the next section, we will obtain a different conclusion when higher order processes in the tunneling expansion are considered.

5. Cotunneling

We first discuss the general approach to consider the cotunneling corrections to the rate equations. Then we show that, in a specific regime, the cotunneling process dominates the total current. Finally, we concentrate on the elastic tunnel current to clarify the differences between the magneto-elastic and polaronic interactions.

5.1. General formula

The explicit form of the transition rates induced by cotunneling processes is given in Appendix B.

Assuming that the phonons are equilibrated, we find that the rate equation (46) including cotunneling events reads

$$(\mathbf{W} + \delta\mathbf{W})(\mathbf{P} + \delta\mathbf{P}) = 0 \tag{65}$$

where $\delta\mathbf{P}$ is a correction to the occupation probabilities $\mathbf{P}$ found in Section 4 (with $\delta P_0 + \delta P_\uparrow + \delta P_\downarrow = 0$),

$$\delta\mathbf{W} = \sum_{\nu,\mu=l,r} \begin{pmatrix} 0 & 0 & 0 \\ 0 & -W_{\uparrow\downarrow}^{(\mu\nu)} & W_{\downarrow\uparrow}^{(\mu\nu)} \\ 0 & W_{\uparrow\downarrow}^{(\mu\nu)} & -W_{\downarrow\uparrow}^{(\mu\nu)} \end{pmatrix} \tag{66}$$

and we introduced the reduced cotunneling rates

$$W_{ss'}^{(\nu\nu')} = \sum_{n,m} P_n^{(\mathrm{eq})} W_{sn,s'm}^{(\nu\nu')} \tag{67}$$

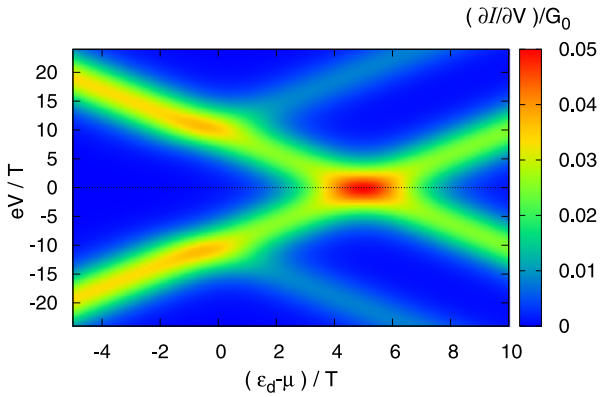

Fig. 2. Differential conductance in the absence of electron–phonon coupling ($\alpha = 0$) as a function of gate and bias voltages in the sequential tunneling regime, for $\mu_B B/T = 5$, $\Gamma_l/T = \Gamma_r/T = 0.1$.

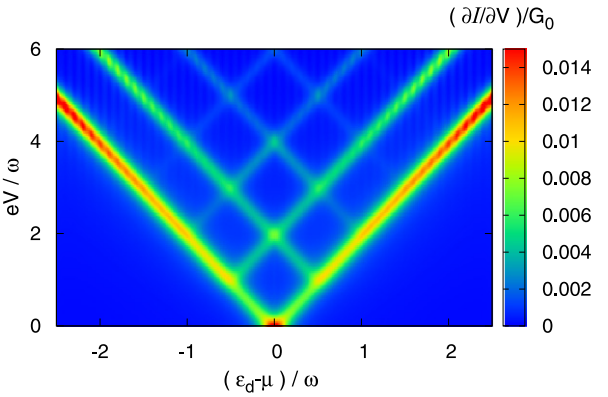

Fig. 3. Differential conductance at zero magnetic field as a function of gate and bias voltages in the sequential tunneling regime, for $\alpha = 1$, $\omega/T = 20$, and $\Gamma_l/T = \Gamma_r/T = 0.1$.

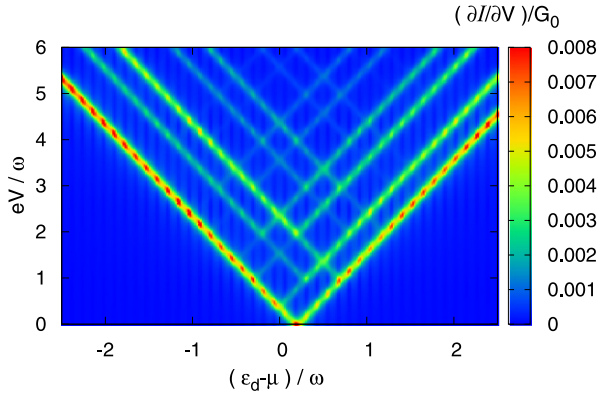

Fig. 4. Differential conductance as a function of gate and bias voltages in the sequential tunneling regime, for $\lambda = 1$, $\phi = 0.4$, $\mu_B B/\omega = 0.2$, $\omega/T = 40$, and $\Gamma_l/T = \Gamma_r/T = 0.1$.

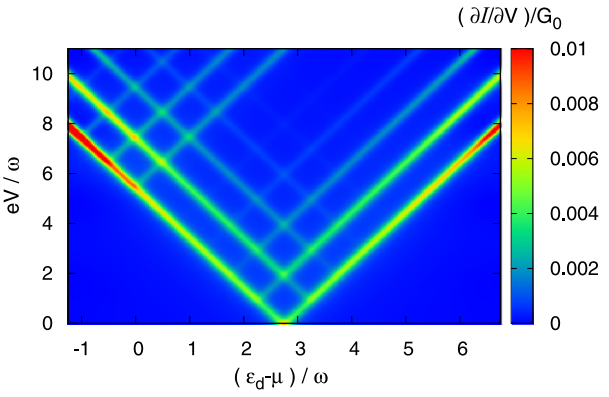

Fig. 5. Differential conductance as a function of gate and bias voltages in the sequential tunneling regime, for $\lambda = 1$, $\phi = 0.4$, $\mu_B B/\omega = 2.75$, $\omega/T = 20$, and $\Gamma_l/T = \Gamma_r/T = 0.1$.

corresponding to the transmission of one electron from lead ν to lead ν' without variation of the dot state, $s = s' = 0, \uparrow, \downarrow$, or with a spin-flip process between $\sigma = \uparrow$ and $\sigma' = \downarrow$.

Considering that the cotunneling rates are smaller than the sequential tunneling rates by a factor $\sim \Gamma/T$, we neglect a term $\delta\mathbf{W}\delta\mathbf{P}$ in Eq. (65) and we find that the correction to the occupation probabilities solves $\mathbf{W}\delta\mathbf{P} = -\delta\mathbf{W}\mathbf{P}$. Note that, when the oscillator is at thermal equilibrium, the cotunneling processes affect the steady occupation probabilities $\mathbf{P}$ only via the spin-flip processes. In the limit of vanishing magnetic field, we have, by symmetry, $W^{(\mu\nu)}_{\uparrow\downarrow} = W^{(\mu\nu)}_{\downarrow\uparrow}$ and $P_\uparrow = P_\downarrow$. Then the cotunneling rates completely cancel from Eq. (65), in agreement with the results of Ref. [16].

According to the previous discussion, the cotunneling correction to the current can be decomposed in two parts:

$$\delta I = \delta I_1 + \delta I_2 \tag{68}$$

They represent respectively the correction to the current due to the electron transfer via cotunneling:

$$\delta I_1 = e\big(W^{(lr)}_{00} - W^{(rl)}_{00}\big)P_0 + e\sum_{\sigma,\sigma'=\uparrow,\downarrow}\big(W^{(lr)}_{\sigma\sigma'} - W^{(rl)}_{\sigma\sigma'}\big)P_\sigma \tag{69}$$

and the effect of the variation of the occupation probabilities produced by the cotunneling processes:

$$\delta I_2 = e\sum_{\sigma}\big(W^{(l)}_{0\sigma}\delta P_0 - W^{(l)}_{\sigma 0}\delta P_\sigma\big) \tag{70}$$

In the next section, we discuss the results for the current.

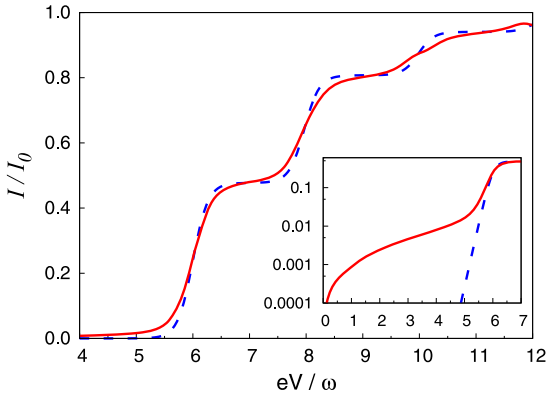

Fig. 6. Bias voltage dependence of the current with (straight line) and without (dashed line) the cotunneling contribution, for $\lambda = 1$, $\phi = 0.4$, $\Gamma_l/T = \Gamma_r/T = 0.4$, $\omega/T = 15$, $(\varepsilon_d - \mu)/\omega = 5$, and $\mu_B B/\omega = 2$. Insert: Zoom of the low-voltage region in log-scale.

5.2. Discussion

The above formalism allows us to obtain the current including both sequential tunneling and cotunneling contributions, for arbitrary parameters of the junction. An example is shown in Fig. 6. In general, cotunneling processes produce a smoothing of the features already discussed in the sequential current, that is the steps associated with the vibrational sidebands and the Zeeman splitting. However they dominate the current in the regions where it is strongly suppressed at the sequential level, see insert of Fig. 6.

In the following, we will concentrate on the region where the cotunneling terms dominate the current. To simplify the expressions for the current, we will further assume that the gate voltage is tuned in the region where the dot is mostly empty ($P_0 \approx 0$) and the magnetic field is sufficiently large that only the down spin state for the singly occupied dot can be accessed virtually, that is when $\varepsilon_d - \mu, \mu_B B \gg T, eV$. In addition, we will consider that $T \ll \omega$ so that the oscillator is in its ground state. Then the expression (68) for the current (noted I instead of δI from now) simplifies to

$$I = e\left(W_{00}^{(lr)} - W_{00}^{(rl)}\right) \tag{71}$$

with

$$W_{00}^{(\nu\nu')} = \frac{\Gamma_\nu \Gamma_{\nu'}}{2\pi} \sum_{m,p,q=0}^{\infty} M_{0q}^{(\nu)*} M_{mq}^{(\nu')} M_{0p}^{(\nu)} M_{mp}^{(\nu')*} \mathcal{F}(\mu_\nu; \mu_{\nu'} + m\omega; \varepsilon_{d\downarrow} + q\omega; \varepsilon_{d\downarrow} + p\omega) \tag{72}$$

where the function $\mathcal{F}$ is defined in Appendix B. A finite electron–phonon interaction results in the suppression of the cotunneling current, compared to the current in the absence of that interaction $I^{(0)} = (I_0 \Gamma/4\pi^2 T)\{\Psi'[1/2 + i(\mu_l - \varepsilon_{d\downarrow})/(2\pi T)] - \Psi'[1/2 + i(\mu_r - \varepsilon_{d\downarrow})/(2\pi T)]\}$, where $I_0 = e\Gamma_l\Gamma_r/\Gamma$. Similarly to the results found in Section 4 we find that the polaronic and magneto-elastic couplings cannot be distinguished close to the charge degeneracy point, at $\varepsilon_{d\downarrow} - \mu \ll \omega$. Focusing for instance on the elastic contribution to the cotunneling current,

$$I = I^{(0)} \left|M_{00}^{(l)}\right|^2 \left|M_{00}^{(r)}\right|^2 = I^{(0)} e^{-2\alpha^2} \tag{73}$$

we find that the suppression factor is the square of the one found in the sequential tunneling regime. This effect can be understood by (i) projecting Hamiltonian (40)–(41) over the oscillator's ground state [25], thus obtaining an effective Hamiltonian for a non-interacting resonant level with renormalized tunneling amplitudes $t_\nu^{\text{eff}} = t_\nu \exp(-\alpha^2/2)$, and (ii) recalling that the current is obtained as a fourth-order effect in these tunneling amplitudes.

Instead, far away from the charge resonance at $\varepsilon_{d\downarrow} - \mu \gg \omega$, we find

$$I = I^{(0)} \sum_{q,p=0}^{\infty} M_{0q}^{(l)*} M_{0q}^{(r)} M_{0p}^{(l)} M_{0p}^{(r)*} = I^{(0)} \left|\langle 0|A_l A_r^\dagger|0\rangle\right|^2 = I^{(0)} e^{-2\phi^2} \tag{74}$$

(here $A_\nu = e^{\alpha_\nu b - \alpha_\nu^* b^\dagger}$), which is only suppressed by the magneto-elastic coupling. The absence of an exponential suppression of the cotunneling current in the polaronic case was noted in Ref. [27]. The magneto-elastic effect can be understood by accounting for the virtual transitions to the singly occupied states of the dot perturbatively [23].

In general, the polaronic and magneto-elastic couplings suppress the cotunneling current in different ways at not too large oscillator's frequency. The difference is traced back to the way the couplings appear in the tunneling Hamiltonian (41). In the polaronic case, an electron crossing the junction is subject to opposite phases $\pm i\lambda(b - b^\dagger)$ at the tunnel barriers with the leads and the dot, which can result in a compensation of their effect. Instead, in the magneto-elastic case the electron

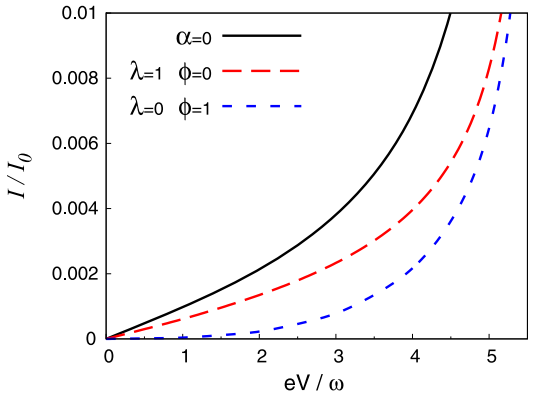

Fig. 7. Bias voltage dependence of the current for different electron–phonon couplings and $\Gamma_l/T = \Gamma_r/T = 0.4$, $\omega/T = 15$, $(\varepsilon_d - \mu)/\omega = 5$, and $\mu_B B/\omega = 2$.

feels the same phase $\phi(b + b^\dagger)$ at each barrier. Indeed, for the same amplitude of the coupling constants, we find that the suppression of the cotunneling current is stronger for the magneto-elastic interaction than for the polaronic interaction, see Fig. 7.

6. Conclusions

In conclusion, we have studied how the quantum vibrations of a suspended carbon nanotube in the quantum dot regime affect the charge transport through it. We have paid special attention to the respective signatures of the polaronic effect that arises from the position-dependent capacitive coupling of the nanotube with a nearby gate and the magneto-elastic coupling in the presence of a transverse magnetic field. While both couplings act similarly in the suppression of the current at the sequential tunneling order, their effect is qualitatively different in the cotunneling regime.

Our estimates for the polaron and magneto-elastic coupling constants show that these effects may be relevant to determine the current–voltage characteristics through suspended nanotubes. Thus, charge transport could be efficiently used to demonstrate the quantum nature of the mechanical vibrations of these tiny objects.

Acknowledgements

This work has been supported by ANR through contract JCJC-036 NEMESIS and by the Nanosciences Foundation (Grenoble). G.R. acknowledges support from the European networks SOLID and GEOMDISS, and from ANR contract QUANTJO.

Appendix A. Rigorous derivation of Eq. (8)

In this appendix, the effectively one-dimensional Hamiltonian (8) for electrons in a suspended nanowire is derived and its conditions of validity are obtained.

For this, we start again with Eq. (1) and then perform a unitary transformation $\mathcal{H} \to e^{iS}\mathcal{H}e^{-iS}$ where $S = p_y u(x) - eBU(x)$, to obtain

$$\mathcal{H} = \frac{[p_x - p_y\partial_x u(x) - eBy]^2 + \boldsymbol{p}_\perp^2}{2m} + V(\boldsymbol{r}) + \sum_n \left(\frac{[P_n - p_y f_n(x) + eBF_n(x)]^2}{2M} + \frac{M\omega_n^2 X_n^2}{2} \right) \tag{A.1}$$

Here $\boldsymbol{p}_\perp = (p_y, p_z)$. Assuming a strong confinement in the nanowire, we project Eq. (A.1) on the ground state for the electron's transverse motion, and we obtain

$$\mathcal{H} \approx \frac{[p_x - eB\langle y\rangle_0]^2}{2m} + \varepsilon_t + V_b(x) + \sum_n \left(\frac{[P_n + eBF_n(x)]^2}{2M} + \frac{M\omega_n^2 X_n^2}{2} + \frac{eB\langle\{y, p_y\}\rangle_0}{2m} X_n f_n'(x) + \frac{\langle p_y^2\rangle_0}{2M} f_n(x)^2 \right) + \frac{\langle p_y^2\rangle_0}{2m} \left(\sum_n X_n f_n'(x) \right)^2 \tag{A.2}$$

with

$$\varepsilon_t = \varepsilon_0 + \frac{e^2B^2}{2m}\left[\langle y^2\rangle_0 - \langle y\rangle_0^2\right] \tag{A.3}$$

In Eqs. (A.2)–(A.3), we denoted $\langle a\rangle_0 = \int d\boldsymbol{r}_\perp \chi_0^* a \chi_0$ for an arbitrary function $a(\boldsymbol{r}_\perp, \boldsymbol{p}_\perp)$, where $\boldsymbol{r}_\perp = (y, z)$ and χ_0 is the ground-state wavefunction for transverse motion that solves the Schrödinger equation:

$$\left[\frac{\boldsymbol{p}_\perp^2}{2m} + U_{\rm conf}(\boldsymbol{r}_\perp)\right]\chi_0(\boldsymbol{r}_\perp) = \varepsilon_0\chi_0(\boldsymbol{r}_\perp) \tag{A.4}$$

(Note that $\langle p_y\rangle_0 = 0$.) The first term in Eq. (A.3) is the ground-state energy ε_0 for transverse motion, the second term is a global diamagnetic shift. Both will be absorbed into the chemical potential from now.

We now argue that the last three terms of Eq. (A.2) can be safely neglected:

The first term would lead to a shift in the equilibrium position of the nanotube that is characterized by a relative displacement $\delta X_n/X_{n0} \sim (M/m)(X_{n0}/L)^2\phi_n$ of the eigenmode n. We also anticipated that the relevant magnetic field dependence in the model enters through flux $\sim BLX_{n0}$, see Eq. (23).

The second term (like the third one) acts even in the absence of magnetic field. It generates an energy shift $\Delta\varepsilon$ when the electron is in the suspended section of the nanowire, with typical amplitude $\Delta\varepsilon/\omega_n \sim (X_{n0}/L_\perp)^2(L/a)$. Here, $L_\perp$ is the transverse width of the wire and a is a cut-off at short distances (on the nanoscale) which regularizes the sum $\sum_n f_n^2(x) = \delta(0)$ that diverges formally in the approximation of continuous medium leading to Eq. (4). The parameter a represents the microscopic atomic distance, the natural length scale at which the continuous model ceases to be valid.

The last term leads to a renormalization of the oscillator's frequency when the electron is in the suspended nanowire, with typical relative magnitude $\delta\omega_n/\omega_n \sim (M/m).(X_{n0}/L)^2.(X_{n0}/L_\perp)^2$. We can check that all terms give small correction in the case of the single-wall carbon nanotube with parameters given in Section 2.4.

Taking into account these simplifications in Eq. (A.2) and making another unitary transformation $\mathcal{H} \to e^{iS'}\mathcal{H}e^{-iS'}$, with $S' = eBx\langle y\rangle_0$, we finally recover Eq. (8).

Appendix B. Transition rates associated with cotunneling events

In this appendix we obtain the transition rates associated with cotunneling events following the method discussed in Ref. [27].

In the absence of sequential tunneling term in Eq. (45), the transition rate (44) for the dot-phonon state to evolve from (s,n) to (s',m) while an electron is transferred from lead ν to lead ν' is

$$\begin{aligned} W^{(\nu\nu')}_{sn,s'm} = {} & 2\pi \sum_{i_\nu, f_\nu} \sum_{i_{\nu'}, f_{\nu'}} P^{(\rm eq)}(i_\nu) P^{(\rm eq)}(i_{\nu'}) \left|\langle f_\nu, f_{\nu'}, s', n| H_T G_0 H_T |i_\nu, i_{\nu'}, s, m\rangle\right|^2 \\ & \times \delta(\Delta E_\nu + \Delta E_{\nu'} + \Delta_{ss'} + \Delta_{mn}) \end{aligned} \tag{B.1}$$

where $\Delta E_\nu = E_{f_\nu} - E_{i_\nu}$, $\Delta_{mn} = \omega[m-n]$, and $\Delta_{ss'} = \varepsilon_{ds} - \varepsilon_{ds'}$.

The non-vanishing rates take the form

$$W^{(\nu\nu')}_{0n,0m} = \frac{\Gamma_\nu\Gamma_{\nu'}}{2\pi}\int {\rm d}\xi\, n_\nu(\xi)\big[1 - n_{\nu'}(\xi + \Delta_{nm})\big] \sum_{\sigma=\uparrow,\downarrow} \left|\sum_{q=0}^{\infty} \frac{M^{(\nu)*}_{nq} M^{(\nu')}_{mq}}{\xi - \varepsilon_{d\sigma} + \Delta_{nq} + i\eta}\right|^2 \tag{B.2}$$

$$W^{(\nu\nu')}_{\sigma n,\sigma' m} = \frac{\Gamma_\nu\Gamma_{\nu'}}{2\pi}\int {\rm d}\xi\, n_\nu(\xi)\big[1 - n_{\nu'}(\xi + \Delta_{\sigma\sigma'} + \Delta_{nm})\big] \left|\sum_{q=0}^{\infty} \frac{M^{(\nu)*}_{qm} M^{(\nu')}_{qn}}{-\xi + \varepsilon_{d\sigma'} + \Delta_{mq} + i\eta}\right|^2 \tag{B.3}$$

These expressions diverge as $\eta \to 0$. A regularization scheme to remove this divergence while the sequential tunneling events are properly taken was discussed in Ref. [27]. It consists in removing an $\mathcal{O}(1/\eta)$-term, which corresponds to sequential tunneling events and is already accounted for in the rates (49), while keeping the next order term [$\mathcal{O}(1)$ term]. On the end, the regularized cotunneling transition rates read

$$W^{(\nu\nu')}_{0n,0m} = \frac{\Gamma_\nu\Gamma_{\nu'}}{2\pi} \sum_{\sigma=\uparrow,\downarrow} \sum_{p,q=0}^{\infty} M^{(\nu)*}_{nq} M^{(\nu')}_{mq} M^{(\nu)}_{np} M^{(\nu')*}_{mp} \mathcal{F}(\mu_\nu; \mu_{\nu'} - \Delta_{nm}; \varepsilon_{d\sigma} - \Delta_{nq}; \varepsilon_{d\sigma} - \Delta_{np}) \tag{B.4}$$

$$W^{(\nu\nu')}_{\sigma n,\sigma' m} = \frac{\Gamma_\nu\Gamma_{\nu'}}{2\pi} \sum_{p,q=0}^{\infty} M^{(\nu)*}_{qm} M^{(\nu')}_{qn} M^{(\nu)}_{pm} M^{(\nu')*}_{pn} \mathcal{F}(\mu_\nu; \mu_{\nu'} - \Delta_{\sigma\sigma'} - \Delta_{nm}; \varepsilon_{d\sigma'} + \Delta_{mp}; \varepsilon_{d,\sigma'} + \Delta_{mq}) \tag{B.5}$$

where

$$\begin{aligned} \mathcal{F}(E_1, E_2, \varepsilon_1, \varepsilon_2) &= \lim_{\eta\to 0} {\rm Re}\left[\int {\rm d}E \frac{n(E-E_1)[1-n(E-E_2)]}{(E-\varepsilon_1+i\eta)(E-\varepsilon_2-i\eta)} - \mathcal{O}\left(\frac{1}{\eta}\right)\right] \\ &= \frac{n_B(E_2-E_1)}{\varepsilon_1-\varepsilon_2}\,{\rm Re}\left[\Psi\left(\frac{1}{2} + i\frac{E_2-\varepsilon_1}{2\pi T}\right) - \Psi\left(\frac{1}{2} + i\frac{E_2-\varepsilon_2}{2\pi T}\right)\right. \\ &\quad \left. - \Psi\left(\frac{1}{2} + i\frac{E_1-\varepsilon_1}{2\pi T}\right) + \Psi\left(\frac{1}{2} + i\frac{E_1-\varepsilon_2}{2\pi T}\right)\right] \end{aligned} \tag{B.6}$$

$n_B(E)$ is the Bose distribution function, and Ψ is the digamma function.

References

[1] H. Park, J. Park, A.K.L. Lim, E.H. Anderson, A.P. Alivisatos, P.L. McEuen, Nano-mechanical oscillations in a single-C60 transistor, Nature 407 (2000) 57.
[2] V. Sazonova, Y. Yaish, H. Ustunel, D. Roundy, A. Arias, P.M. McEuen, A tunable carbon nanotube electromechanical oscillator, Nature 431 (2004) 284.
[3] A.K. Huettel, G.A. Steele, B. Witkamp, M. Poot, L.P. Kouwenhoven, H.S.J. van der Zant, Carbon nanotubes as ultrahigh quality factor mechanical resonators, Nano Lett. 9 (2009) 2447.
[4] B. Lassagne, Y. Tarakanov, J. Kinaret, D. Garcia-Sanchez, A. Bachtold, Coupling mechanics to charge transport in carbon nanotube mechanical resonators, Science 325 (2009) 1107.
[5] G.A. Steele, A.K. Huettel, B. Witkamp, M. Poot, B. Meerwaldt, L.P. Kouwenhoven, H.S.J. van der Zant, Strong coupling between single-electron tunneling and nanomechanical motion, Science 325 (2009) 1103.
[6] B.J. LeRoy, S.G. Lemay, J. Kong, C. Dekker, Scanning tunneling spectroscopy of suspended single-wall carbon nanotubes, Appl. Phys. Lett. 84 (2004) 4280.
[7] R. Leturcq, C. Stampfer, K. Inderbitzin, L. Durrer, C. Hierold, E. Mariani, M.G. Schultz, F. von Oppen, K. Ensslin, Franck–Condon blockade in suspended carbon nanotube quantum dots, Nat. Phys. 5 (2009) 327.
[8] L.I. Glazman, R.I. Shekhter, Inelastic resonant tunneling of electrons through a potential barrier, Soviet Phys. – JETP 67 (1) (1988) 163.
[9] N.S. Wingreen, K.W. Jacobsen, J.W. Wilkins, Inelastic scattering in resonant tunneling, Phys. Rev. B 40 (17) (1989) 11834–11850.
[10] D. Boese, H. Schoeller, Influence of nanomechanical properties on single-electron tunneling: A vibrating single-electron transistor, Europhys. Lett. 54 (2001) 668.
[11] K.D. McCarthy, N. Prokof'ev, M.T. Tuominen, Incoherent dynamics of vibrating single-molecule transistors, Phys. Rev. B 67 (2003) 245415.
[12] S. Braig, K. Flensberg, Vibrational sidebands and dissipative tunneling in molecular transistors, Phys. Rev. B 68 (2003) 205324.
[13] A. Mitra, I. Aleiner, A.J. Millis, Phonon effects in molecular transistors: Quantal and classical treatment, Phys. Rev. B 69 (2004) 245302.
[14] A. Zazunov, D. Feinberg, T. Martin, Phonon-mediated negative differential conductance in molecular quantum dots, Phys. Rev. B 73 (11) (2006) 115405.
[15] R. Egger, A.O. Gogolin, Vibration-induced correction to the current through a single molecule, Phys. Rev. B 77 (2008) 113405.
[16] J. Koch, F. von Oppen, Franck–Condon blockade and giant Fano factors in transport through single molecules, Phys. Rev. Lett. 94 (2005) 206804.
[17] C.B. Doiron, W. Belzig, C. Bruder, Electrical transport through a single-electron transistor strongly coupled to an oscillator, Phys. Rev. B 74 (2006) 205336.
[18] D. Mozyrsky, M.B. Hastings, I. Martin, Intermittent polaron dynamics: Born–Oppenheimer approximation out of equilibrium, Phys. Rev. B 73 (3) (2006) 035104.
[19] F. Pistolesi, S. Labarthe, Current blockade in classical single electron nano-mechanical resonator, Phys. Rev. B 76 (2007) 165317.
[20] F. Pistolesi, Ya.M. Blanter, I. Martin, Self-consistent theory of molecular switching, Phys. Rev. B 78 (8) (2008) 085127.
[21] G. Weick, F. Pistolesi, E. Mariani, F. von Oppen, Discontinuous Euler instability in nanoelectromechanical systems, Phys. Rev. B 81 (2010) 121409.
[22] G. Weick, F. von Oppen, F. Pistolesi, Euler buckling instability and enhanced current blockade in suspended single-electron transistors, Phys. Rev. B 83 (2011) 035420.
[23] R.I. Shekhter, L.Y. Gorelik, L.I. Glazman, M. Jonson, Electronic Aharonov–Bohm effect induced by quantum vibrations, Phys. Rev. Lett. 97 (2006) 156801.
[24] G. Sonne, Temperature-independent current deficit due to induced quantum nanowire vibrations, New J. Phys. 11 (7) (2009) 073037.
[25] G. Rastelli, M. Houzet, F. Pistolesi, Resonant magneto-conductance of a suspended carbon nanotube quantum dot, EPL (Europhys. Lett.) 89 (5) (2010) 57003.
[26] G.A. Skorobagatko, S.I. Kulinich, I.V. Krive, R.I. Shekhter, M. Jonson, Magnetopolaronic effects in electron transport through a single-level vibrating quantum dot, Low Temp. Phys. 37 (2011) 1295.
[27] J. Koch, F. von Oppen, A.V. Andreev, Theory of the Franck–Condon blockade regime, Phys. Rev. B 74 (20) (2006) 205438.
[28] F. Pistolesi, Cooling a vibrational mode coupled to a molecular single-electron transistor, J. Low Temp. Phys. 154 (2009) 199–210.
[29] L.D. Landau, E.M. Lifshitz, Theory of Elasticity, Elsevier, 1986.
[30] S. Sapmaz, Ya.M. Blanter, L. Gurevich, H.S.J. van der Zant, Carbon nanotubes as nanoelectromechanical systems, Phys. Rev. B 67 (2003) 235414.
[31] K. Flensberg, Electron–vibron coupling in suspended nanotubes, New J. Phys. 8 (1) (2006) 5.
[32] A. Zazunov, T. Martin, Transport through a molecular quantum dot in the polaron crossover regime, Phys. Rev. B 76 (3) (2007) 033417.
[33] L. Mühlbacher, E. Rabani, Real-time path integral approach to nonequilibrium many-body quantum systems, Phys. Rev. Lett. 100 (2008) 176403.
[34] A.S. Alexandrov, A.M. Bratkovsky, Memory effect in a molecular quantum dot with strong electron–vibron interaction, Phys. Rev. B 67 (2003) 235312.
[35] J.-C. Charlier, X. Blase, S. Roche, Electronic and transport properties of nanotubes, Rev. Mod. Phys. 79 (2007) 677–732.
[36] H.T. Imam, V.V. Ponomarenko, D.V. Averin, Coulomb blockade of resonant tunneling, Phys. Rev. B 50 (1994) 18288–18298.
[37] L.I. Glazman, K.A. Matveev, Coulomb correlations in the tunneling through resonance centers, JETP Lett. 48 (1988) 445.